Direct and indirect effects of precipitation on Particulate Matter concentrations in the Aburrá Valley

Natalia Roldán Henao

Tesis presentada como requisito parcial para optar al título de:

Profesional en Ingeniría Ambiental

Director:

Carlos David Hoyos PhD.

Línea de Investigación:

Ciencias de la tierra y del espacio - Meteorologıa

Universidad Nacional de Colombia

Facultad de Minas, Escuela de Geociencias y Medio Ambiente

Medellín, Colombia

2017

Abstract

Precipitation modulates pollutant concentration in the atmosphere directly and indirectly trough different mechanisms. Wet deposition, including in-cloud scavenging and below-cloud scavenging (BCS), is one of the main drivers of particulate matter removal from the atmosphere. Our focus is to assess, using observations, a non-parametric conditional analysis, and the signed overlapping coefficient complement index, the net effect of precipitation on pollutant concentration considering not only the direct near-surface aerosol BCS but also the indirect effect associated with the induced lower troposphere stability limiting the vertical dispersion, leading to pollutant concentration increase. We consider precipitation effects on PM2.5, PM10, NO_2, and ozone. Probability Density Functions (PDF) of pollutant concentration during precipitations events and under dry conditions are analyzed for every hour of the day. The net effect of precipitation on PM2.5, PM10 are NO_2 concentration is strongly dependent on the atmospheric stability. During the nighttime and before midmorning the atmosphere is stable; a precipitation event during this time generates BCS reducing the concentration of particulate matter in the atmosphere. During afternoon, unstable atmospheric conditions are predominan and aerosols disperse vertically; a precipitation event during this period stabilizes the atmosphere, generating early stratification which, together with then continued anthropogenic emissions during the day, lead to near-surface pollutant accumulation, offsetting the washout effect of precipitation. Similar results are obtained for NO_2 during the afternoon. In the case of ozone; reduced radiation inhibits the formation of ozone in the afternoon.

1 Introduction

During the last decades, atmospheric pollution has become one of the foremost environmental concerns for expanding metropolitan areas around the globe. The population and economic growth, the increase in energy demand, and the transportation models, have led to the rise of pollutant emissions into the atmosphere, worsening air quality conditions in urban areas [Mayer, 1999, Li et al., 2015]. In megacities such as New Delhi (India), and Beijing (China), extreme air pollution episodes are experienced frequently with hourly fine particulate matter (PM2.5) concentrations exceeding 400 μgm^{-3} [Yang et al., 2015, Marlier et al., 2016], and annual concentrations above 90 μgm^{-3} [Cheng et al., 2016]. The air quality problem is widespread globally, and it is part of the ecology of cities where pollution generation outpaces societal capacity to implement control measures [Grimm et al., 2008]. Expanding urban areas in tropical regions have not escaped the deterioration of air quality; on the contrary, often complex topography combined with highly variable climate conditions exacerbates this challenge. In the last five years, the city of Medellín (see Figure **1-1**a), Colombia, has experienced the onset of critical environmental episodes characterized by poor air quality, and in particular, sudden peaks of fine particulate matter concentration. The increment in the number of emission sources, in particular, mobile sources (see Figure **1-1**b), led to a long-term increase in PM2.5 before 2016, exacerbated by critical episodes associated with lower-troposphere stability. The combination of growing emissions, complex topography, and unfavorable climate and meteorological conditions for vertical dispersion of pollutants triggered PM2.5 concentrations to peak during March 2016 (see Figure **1-1**c), with hourly particulate matter reaching up to 180 μgm^{-3}, daily concentrations of 118 μgm^{-3}, and 22

days of unhealthy air quality conditions according to the Environmental Protection Agency (EPA) standards.

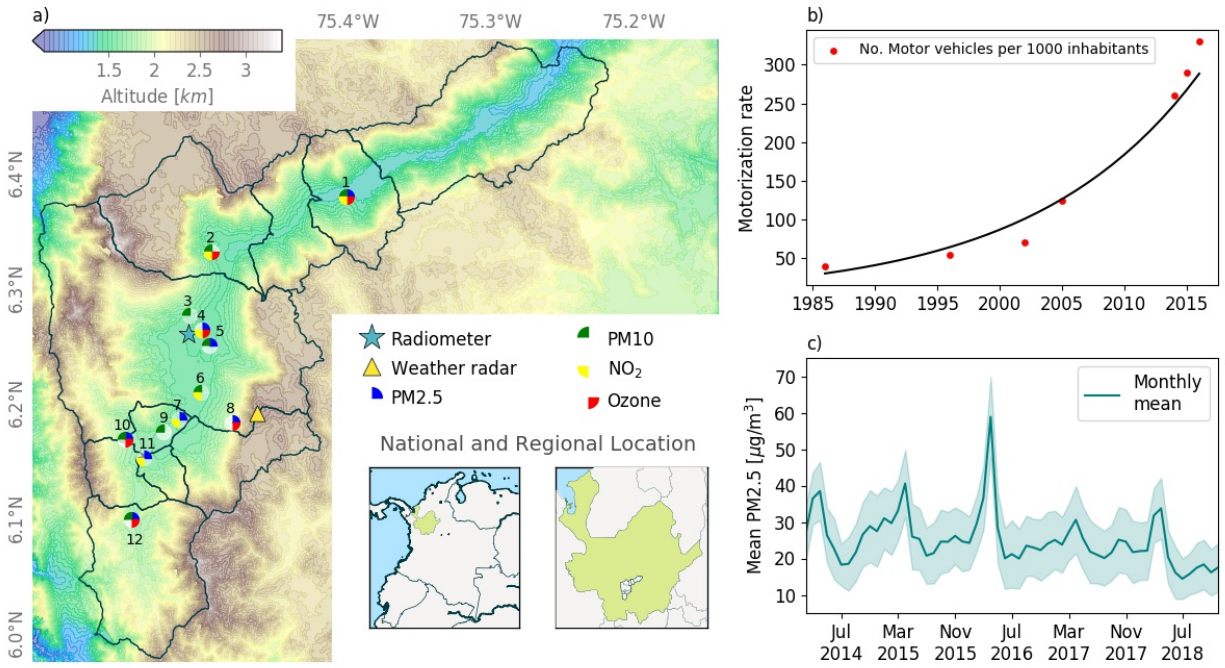

Figura 1-1: a) Geographical context of the Aburrá Valley, located in Colombia, Department of Antioquia. The map shows, in blue to brown colors, the main topographic features of the region and the distribution of the air quality monitoring stations, the microwave radiometer and the weather radar. In the study we use the following monitoring stations: eight in-situ PM2.5, eight PM10, six ozone, and six NO_2. b) Yearly evolution of the motorization rate in the Aburrá valley. The motorization rate corresponds to the number of vehicles per 1000 people. c) Monthly evolution of average PM2.5 concentration in the Aburrá Valley. The spatial average is computed using eight PM2.5 stations. The period of the PM2.5 records is from January 2014 to March 2018. The shadow corresponds to mean value +/- one standard deviation representing the variability.

Several studies indicate that exposure to high concentrations of particulate matter, or during

extended periods of time, can contribute to, or even cause, respiratory, cardiovascular and cognitive diseases [Anderson et al., 2012, Brunekreef and Holgate, 2002, Lelieveld et al., 2015, Newby et al., 2015, Münzel et al., 2017, Zhang et al., 2018]. Lelieveld et al. [2015] suggested that during 2010 approximately 3.3 million premature deaths worldwide were attributable to high concentrations of PM2.5, and according to model projections, this number could double by 2050. Recent evidence suggests that overall atmospheric pollution was likely responsible for an estimated 9 million premature deaths during 2015 [Landrigan et al., 2017].

In addition to anthropogenic emissions, climate and meteorological conditions also modulate air pollution locally: Stagnant atmospheres and thin planetary boundary layers contribute to the onset of critical air pollution episodes, by controlling whether pollutants are dispersed in the atmosphere or interact among themselves and with water vapor and radiation to form secondary pollutants [Lazaridis, 2011, Elminir, 2005]. Vertical pollutant dispersion during convective conditions, horizontal advection removal, and precipitation scavenging are the meteorological processes that act to remove gaseous pollutants and suspended particles from the near surface atmosphere. In the case of particulate matter, wet deposition is arguably the most important removal route, including rainout, or in-cloud scavenging, and washout or below-cloud scavenging, BCS [Lazaridis, 2011]. In-cloud scavenging corresponds to the incorporation of pollutants within cloud droplets by condensation during the nucleation phase and incorporation of gases surrounding the droplets by aqueous-phase reactions [Chatterjee et al., 2010, Seinfeld and Pandis, 2012, Feng, 2007]. Collisions and coalescence among particulate matter and rain droplets during the fall, or through turbulent and Brownian diffusion, lead to BCS [Duhanyan and Roustan, 2011, Feng, 2007, Zikova and Zdimal, 2016]. Understanding the wet removal processes implies considering multiple scales, from the microscale (10^{-6} m) to the macroscale (10^{6} m), making wet deposition one of the most complex atmospheric processes [Seinfeld and Pandis, 2012, Pruppacher and Klett, 2012].

Most studies on wet deposition have mainly focused on investigating the washout effects by raindrops using a microphysical framework through analysis of the raindrop size distribution, the terminal velocity of raindrops, and the BCS coefficient for particulate pollutants [Chate

and Pranesha, 2004, Chate et al., 2011, Bae et al., 2012, Andronache and Hill, 2003, Wang et al., 2010]. These studies focus on the effectiveness of the washout of solids particles with a specific size under particular rainfall conditions [Olszowski, 2016, Zikova and Zdimal, 2016, Kyrö et al., 2009]. Typically the wet deposition theory considers different types of hydrometeors including rain, haze, and snow, in a wide range of diameters: ultrafine, fine and coarse particles. The washout efficiency is usually evaluated through the scavenging coefficient, on a daily timescale. However, the scavenging coefficient is not easy to estimate due to the complex set of microphysical parameters needed, and therefore an approach linking air quality to observable meteorological parameters such as rainfall is required. Recent studies have evaluated the washout effect in particulate matter concentrations following different approaches than the traditional microphysical framework. Blanco-Alegre et al. used in-situ high temporal resolution rainfall and aerosol measurements to estimate scavenging coefficients, finding aerosol-size and raindrop-size dependent scavenging after precipitation. Guo et al. [2016] used data from two Chinese cities (Guangzhou and Xi'an) to assess the effect of rainfall on aerosol concentration, finding a minimum precipitation threshold, different for both cities, for which air quality improves after the rainfall event. Feng and Wang [2012] computed the precipitation-driven scavenging rate as a measure of the difference in the particle concentration before and after precipitation; their results suggest that, in some cases, factors such as local emissions or atmospheric diffusion conditions are higher than the wet scavenging caused by raindrops, counteracting the washout effect, thus resulting in higher fine particle concentration after a precipitation event. Feng and Wang [2012] stated that low amounts of precipitation had very little influence on the concentrations of all kinds of particles. Guo et al. [2014] also found that artificial rain interventions may worsen air quality under some scenarios.

Vertical dispersion and rainfall-triggered aerosol removal are especially determinant in narrow valleys such as the Aburrá Valley, where the complex topography limits the horizontal dispersion since the magnitude of surface winds is usually very weak. Thus, atmospheric stability conditions and the evolution of the atmospheric boundary layer, and in particular the development of a deep convective layer are considered determining factors in pollutants

concentrations in the Aburrá Valley, as they establish the efficiency of vertical dispersion processes (Herrera and Hoyos 2019). Stable atmospheres inhibit atmospheric vertical exchanges and favor pollutant accumulation, while unstable, convective environments promote pollutants dispersion and mixing [Whiteman, 2000]. In general, atmospheric instability in the Aburrá Valley occurs between 10:00 and 17:00 LT, favoring thermal convection and mixing, triggering vertical dispersion of pollutants. On the other hand, stable conditions are dominant between 19:00 and 09:00 LT (Herrera and Hoyos 2019).

Wet deposition is the only other potential mechanism to remove pollutants from the Aburrá Valley's atmosphere. Figure **1-2**a shows the relationship between total daily precipitation and the 24-hour average PM2.5 in the Aburrá Valley (station 8 in Figure **1-1**). At first glance, the figure shows that high 24-hour PM2.5 concentrations (over 30 $\mu g \mathrm{m}^{-3}$) are more likely to occur when the total daily precipitation is less than 25 mm; however, the observed relationship is not deterministic, it is far from being linear, and it is certainly not as expected based on theoretical scavenging studies. On the contrary, the data points to the potential existence of a relationship in the sense of a necessary but not sufficient condition in which high PM2.5 concentrations are not likely in days with high cumulative precipitation, but low precipitation is not necessarily related with high PM2.5 concentration.

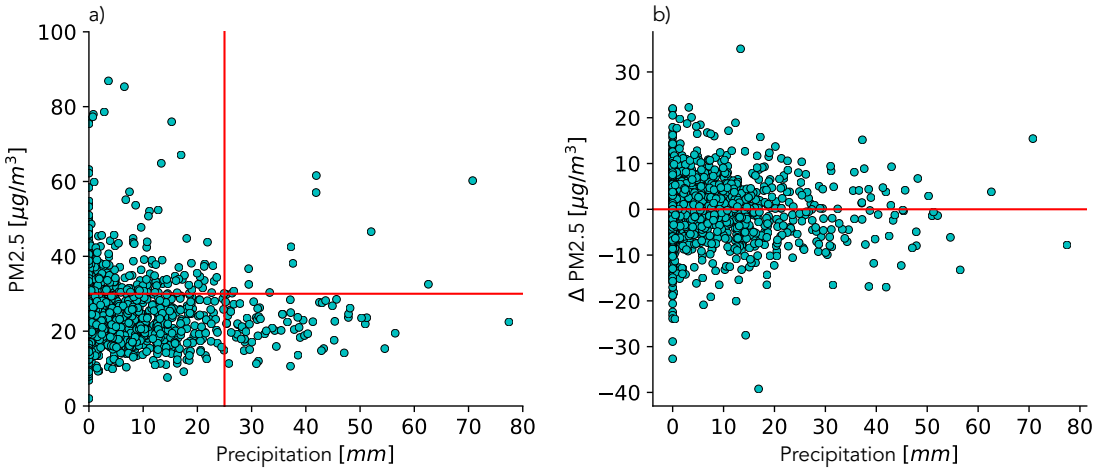

Figura 1-2: a) Scatter plot of daily precipitation and 24 hour-average PM2.5. b) Scatter plot of daily precipitation of daily precipitation and the 24-hour change in PM2.5 concentration.

Notwithstanding the precipitation and 24-hour PM2.5 relationship indicating that, typically, high precipitation leads to low 24-hour PM2.5, the practical utility of this apparent relationship is limited, especially if we consider the predictability and prediction of PM2.5 concentration using rainfall as a predictor variable. The critical issue regarding predictability is whether PM2.5 concentrations can be predicted based on information regarding the cumulative precipitation, or whether small-scale processes that are not predictable dominate the concentration of pollutants in the lower troposphere. Figure **1-2** shows a scatterplot of daily precipitation and the daily change in PM2.5 concentrations (ΔPM2.5) estimated as the 24-hour concentration during the rainy day minus the previous day concentration. The evidence suggests there is no clear reduction of PM2.5 (negative ΔPM2.5) even in cases of large precipitation. On the contrary, there is a considerable number of instances where ΔPM2.5 is positive stressing the fact that the overall direct and indirect precipitation-aerosol concentration relationship is complex.

The focus of the present study is to estimate, using in-situ observations, weather radar

precipitation, and atmospheric thermodynamic profiles, the net effect of precipitation on pollutant concentration under the general hypothesis that it depends not only on the washout efficiency but also on the rainfall-induced stabilization of the lower troposphere. In that sense, and given that the atmospheric stability in the tropics has a strong diurnal cycle induced by the surface energy balance rather than a marked seasonality, it is necessary to examine the net effect in a sub-daily scale. The proposed approach follows a non-parametric conditional analysis of the fine (PM2.5) and coarse (PM10) particulate matter, nitrogen dioxide (NO_2), and ozone (O_3) in an hourly timescale, given different precipitation scenarios. The following section includes the description of the region of study, the main data sets used, the definition of the thermodynamic indices to evaluate lower-troposphere stability, and the conditional analysis based on the estimation of an overlapping coefficient among conditional probability density functions (PDFs). The third section presents the main results of the methodology for pollutant concentration during wet and dry conditions in the Aburrá Valley. Finally, the last section presents the most important conclusions of the study.

2 Data and Methodology

The observational and conditional assessment of the net effect of precipitation on the pollutant concentration presented in this work relies on in-situ air quality measurements from the Aburrá Valley network, rainfall from weather radar quantitative precipitation estimation (radar-based QPE), and thermodynamic indices derived from microwave radiometer retrievals. The Medellín metropolitan area includes ten municipalities settled within the Aburrá Valley, a complex narrow valley, with steep hills, located in northern South America, in the central branch of the Andean mountain range ($6°15'06''N$, $75°33'48''W$). The Aburrá Valley is home to about three and a half million people living in an area of 1152 km^2; the valley is 64 km long and the widest cross-section, from divide to divide, is about 18.2 km wide. The height difference between the top and the bottom of the valley is about 1.4 km.

2.0.1 Data Sources

Particulate matter and gaseous concentrations in the Aburrá Valley are routinely monitored by the local early warning system (Sistema de Alerta Temprana -SIATA-, www.siata.gov.co), a science and technology project established by the local environmental authority (Area Metropolitana del Valle de Aburrá, AMVA). In this work, we consider pollutant records longer than three years to guarantee statistically significant results. Figure **1-1**a shows the spatial distribution of the air-quality monitoring network instruments used in this research and Table **2-1** summarizes the period of the data record used in each case.

Radar-based QPE follows a technique developed by Sepúlveda and Hoyos (2019) using radar reflectivity, disdrometer, and rain gauge information. The radar QPE technique allows the estimation of precipitation maps over the valley and the locations of interest using retrievals from a the Aburrá Valley weather radar, a C-band polarimetric and Doppler radar operated by SIATA. The radar scanning strategy allows obtaining precipitation information every five minutes with a spatial resolution of about 128 m from a 1 degree tilt plan position indicator sweep; the uncertainty associated to QPE is relatively low in a 120 km radius from the installation site. This research uses precipitation products in the period from January 2012 to September 2017.

Thermodynamic indices are estimated from temperature and humidity profiles measured by the MWR (Radiometrics MP-3000A) operated by SIATA. The MWR is located at the top of the SIATA main operations center on the valley floor (see Figure **1-1**), about 60 m from the surface, and provides vertical profiles of the thermodynamic state of the atmosphere with variable spatial resolution: 50 m from the surface to 500 m, 100 m up to 2 km, and 250 m up to 10 km. Thermodynamic profiles are available with a 2-minute time resolution, and the data record spans from January 2013 to September 2017. Specifically, Convective Inhibition Energy (CINE) and the Lifted Index (LI) are considered as proxies of atmospheric stability. CINE indicates the amount of energy that inhibits the updraft of air parcels [Peppler, 1988, Curry and Webster, 1999], and it is an indirect measure of the lower troposphere stability: as the atmosphere becomes stable, CINE becomes more negative. Conversely, unstable atmospheres correspond to values of CINE close to zero. CINE is estimated as follows

$$CINE = \int_{SFC}^{LFC} g\frac{T_v' - T_v}{T_v}dz$$

where LFC is the Level of Free Convection, SFC is the surface layer, T_v is the virtual temperature of the environment and T_v' is the virtual temperature of the parcel [Peppler, 1988]. LI is also a proxy of atmospheric stability: as the atmosphere becomes more unstable, the index tends to be increasingly negative. LI is calculated as

$$LI = T_{500} - T_{500}'*$$

where T_{500} is the environment temperature at 500 hPa and $T'_{500}*$ is the temperature of an air parcel lifted adiabatically from 50hPa above the surface to 500hPa [Peppler, 1988].

2.0.2 Diurnal Cycle Conditional Analysis

One of the most prominent challenges in the assessment of the net effect of precipitation scavenging atmospheric pollutants in a tropical environment is the determination of the appropriate time scale for the analysis. We argue that using daily cumulative precipitation for the study masks the actual net effect of rainfall in aerosol concentration. The 24-hour time scale is artificial and does not distinguish well among the physical processes that lead to precipitation. In the Aburrá Valley, the diurnal cycle of precipitation is bimodal, with intense and short-lived (30-50 minutes) convective rainfall events in the afternoon (14:00 to 17:00 LT), and low-intensity, long-lived stratiform precipitation during the night (00:00 to 04:00 LT). The hypothesis behind the work presented in this study is three-fold: (i) The net effect of rainfall on pollutant concentration depends not only on the efficiency of the washout effect but also on the role of rainfall stabilizing the atmosphere, thus leading to near-surface pollutant accumulation, (ii) the effect of precipitation modulating atmospheric stability has a strong diurnal cycle, and (iii) the time scale for the analysis must allow considering intra-day variability. Here we use hourly resolution datasets, separating the entire record in different categories (48): for each hour of the day, and for dry (precipitation $<$ 2mm per hour) and wet (precipitation $\geq$ 2mm per hour) conditions (24x2). The analysis for wet cases considers pollutant concentrations one hour after the precipitation event to assess the immediate precipitation net effect.

The methodology includes a conditional analysis, contrasting among the different times of the day and among dry and wet conditions, the estimated probability density functions (PDFs) of various atmospheric pollutants similar as the methodology in Agudelo et al. [2011]. This allows examining, in a probabilistic sense, the net effect of precipitation on pollutant concentrations for different hours of the day. The separation of the PDFs for different atmospheric

pollutants, under wet and dry conditions, is a measure of the net effect of precipitation on near-surface pollution, and at the same time a quantitative estimation of the relative net removal efficiency for the different pollutants, and a proxy for the discriminating potential (or predictability) of pollutant concentration based on hourly rainfall data or weather forecasts.

The same procedure is also followed for both thermodynamic indices to analyze the atmospheric stability for dry conditions and after precipitation events, for every hour of the day. Additionally, the net effect of precipitation on pollutant concentration is also studied taking into account the role of intensity, using the same conditional approach. For this assessment, the maximum precipitation intensity is computed for events with cumulative rainfall greater than 5 mm within a 60-minute period; hourly pollutant records are then reclassified in two sets, for precipitation intensities below and above the median.

2.0.3 Overlapping Coefficient

Once all the pollutant PDFs are estimated for each hour of the day, and for wet and dry conditions, we propose using an index to summarize the results estimating the relative separation or agreement among PDFs [Inman and Bradley, 1989]. The index is based on the overlapping coefficient (OC), which corresponds to the area of intersection among PDFs. Let $f_1(x)$ and $f_2(x)$ be the pollutant PDFs for wet and dry conditions; the OC in the discrete case is calculated as follows

$$OC = \sum_x min[f_1(x), f_2(x)]$$

with $0 \leq OC \leq 1$. The index corresponds to the signed OC complement (SOCC) defined as follows

$$SOCC = \begin{cases} OC - 1 & \text{median}\{P(t)|WC\} \leq \text{median}\{P(t)|DC\} \\ 1 - OC & \text{median}\{P(t)|WC\} > \text{median}\{P(t)|DC\} \end{cases}$$

where $P(t)$ represents a given atmospheric pollutant, and WC and DC wet and dry conditions, respectively, with $-1 \leq SOCC \leq 1$; $f_1(x) = \{P(t)|WC\}$ and $f_3(x) = \{P(t)|DC\}$. According to the definition, a SOCC index close to 0 indicates that both distributions share a greater amount of area suggesting, in consequence, that precipitation does not play a significant role in modulating the net pollutant concentration. On the other hand, a SOCC index close to +/- 1 indicates PDFs are more separated, suggesting precipitation is an important discriminating factor altering the pollutant concentration. Negative values of SOCC index correspond to a decrease in pollutant concentrations associated with rainfall and positive values are associated with an increase in pollutant concentrations.

Finally, the non-parametric Wilcoxon-Mann-Whitney test [Mann-Whitney, 1947, Depuy et al., 2014] is used to assess whether the two samples $f_1(x)$ and $f_2(x)$ likely originate from the same distribution. The Wilcoxon-Mann-Whitney test does not assume normality nor equal variance like the T-test and uses the ranks of the data rather than their raw values. In the Wilcoxon-Mann-Whitney test, the null hypothesis is that the distributions of populations $f_1(x)$ and $f_2(x)$ are identical. The statistic for Wilcoxon-Mann-Whitney test is computed as

$$U_1 = n_1 n_2 + \frac{n_1(n_1+1)}{2} - R_1$$
$$U_2 = n_1 n_2 + \frac{n_2(n_2+1)}{2} - R_2$$

where n_1 is the sample size of $\{P(t)|WC\}$ (sample 1), n_2 is the sample size of $\{P(t)|DC\}$ (sample 2), and R_1 and R_2 are the sum of the ranks in samples 1 and 2, respectively. R_1 and R_2 are obtained after ranking all the $n_1 + n_2$ observations in a single sample $\{P(t)|WC\} \cup \{P(t)|DC\} = P(t)$. The normalized test statistic Z, which is approximately Gaussian for large samples, is defined as

$$Z = \frac{U - m_U}{\sigma_U}$$

where $m_U = n_1 n_2/2$, and $\sigma_U = \sqrt{n_1 n_2 (n_1 + n_2 + 1)/12}$. If $|Z|$ is greater than a predetermined cutoff value then the null hypothesis can be rejected. We use 95% significance as a threshold to reject the null hypothesis.

Tabla 2-1: Dates between which, data was taken for pollutants

Station	Type	Initial date	End date
4*1	PM2.5	2013/01/01	2017/09/10
	PM10	2013/01/01	2017/09/10
	NO_2	2015/09/15	2017/09/10
	Ozone	2015/09/04	2017/09/10
3*2	PM10	2013/01/01	2017/09/10
	NO_2	2013/01/01	2017/09/10
	Ozone	2013/01/01	2017/09/10
3	PM10	2013/01/01	2017/09/10
3*4	PM2.5	2013/01/01	2017/09/10
	NO_2	2013/01/01	2017/09/10
	Ozone	2013/01/01	2017/09/10
2*5	PM2.5	2013/01/01	2017/09/10
	PM10	2015/09/09	2017/09/10
2*6	PM10	2013/01/01	2017/09/10
	NO_2	2013/07/01	2017/09/10
2*7	PM2.5	2013/01/01	2017/09/10
	NO_2	2013/01/01	2017/09/10
2*8	PM2.5	2015/09/16	2017/09/10
	Ozone	2015/09/22	2017/09/10
9	PM10	2013/01/01	2017/09/10
3*10	PM2.5	2013/01/01	2017/09/10
	PM10	2013/01/01	2017/09/10
	Ozone	2013/01/01	2017/09/10
2*11	PM2.5	2014/02/04	2017/09/10
	NO_2	2014/02/04	2017/09/10
3*12	PM2.5	2013/01/01	2017/09/10
	PM10	2013/01/01	2017/09/10
	Ozone	2013/01/01	2017/09/10

3 Results

Recurring contrasting evidence of the net effect of rainfall on aerosol concentration is observed after precipitation episodes in the region. As an example, a precipitation event took place on August 24, 2016, from 13:00 to 17:30 LT, over the Medellín metropolitan area (see Figures **3-1**a to d). Subsequently, after the otherwise unassuming rainfall event, PM2.5 concentrations considerably increased as shown in Figure **3-1**e, doubling from an average of around 30 μgm^{-3} in the morning hours to around 60 μgm^{-3} after 15:00 LT. A contrasting case occurred as a result of the nighttime precipitation on March 22, 2017, after which PM2.5 concentrations decreased considerably (see Figure **3-2**). The air quality monitoring network registered PM2.5 concentrations above 60 μgm^{-3} in all ground stations prior to the precipitation event; after the event, the PM2.5 concentrations declined to less than 10 μgm^{-3}.

This contrasting behavior is not episodical. Figure **3-3**a presents the PM2.5 concentration PDFs for wet (blue line) and dry (orange line) conditions in monitoring station 4 in Figure **1-1** at 02:00 LT, showing that, at this time of the day, the likelihood of having lower PM2.5 concentrations is considerably larger after precipitation takes place as a result of aerosol washout. Figure **3-3**b shows the results obtained for the same measuring station at 14:00 LT. In this timeframe, on the contrary, the likelihood of having higher PM2.5 concentrations increases immediately after rainfall events compared to dry days. Clearly, the net effect of precipitation on aerosol concentration is modulated by other factors in addition to the rainfall-induced washout. Similarly, Figure **3-3**c and d show the same analysis as in Figure **3-3**a and b but for PM10 and for monitoring station 5 in Figure **1-1**. Precipitation net effects on PM10 concentration are congruent with the findings for PM2.5.

The previous results suggest there is a diurnal modulation of the net effect of precipitation on aerosol concentration. Figure **3-4** expands the assessment to the entire diurnal cycle, and summarizes the previous distributions using the SOCC index, with negative values indicating a net precipitation-induced aerosol removal, and positive ones suggesting that precipitation leads to pollution accumulation. Results for PM2.5 are presented in Figure **3-4**a, and for PM10 in Figure **3-4**b, for the same monitoring stations as in Figure **3-3**. The most striking result is that the SOCC index changes sign during the day, with negative values during the night and before midmorning, and positive values during the day. In the figure, full green circles correspond to the cases where the null hypothesis, indicating that the distributions of pollutants for wet and dry conditions are identical, can be rejected using the Wilcoxon-Mann-Whitney test. Conversely, white circles correspond to hours in which the null hypothesis cannot be rejected.

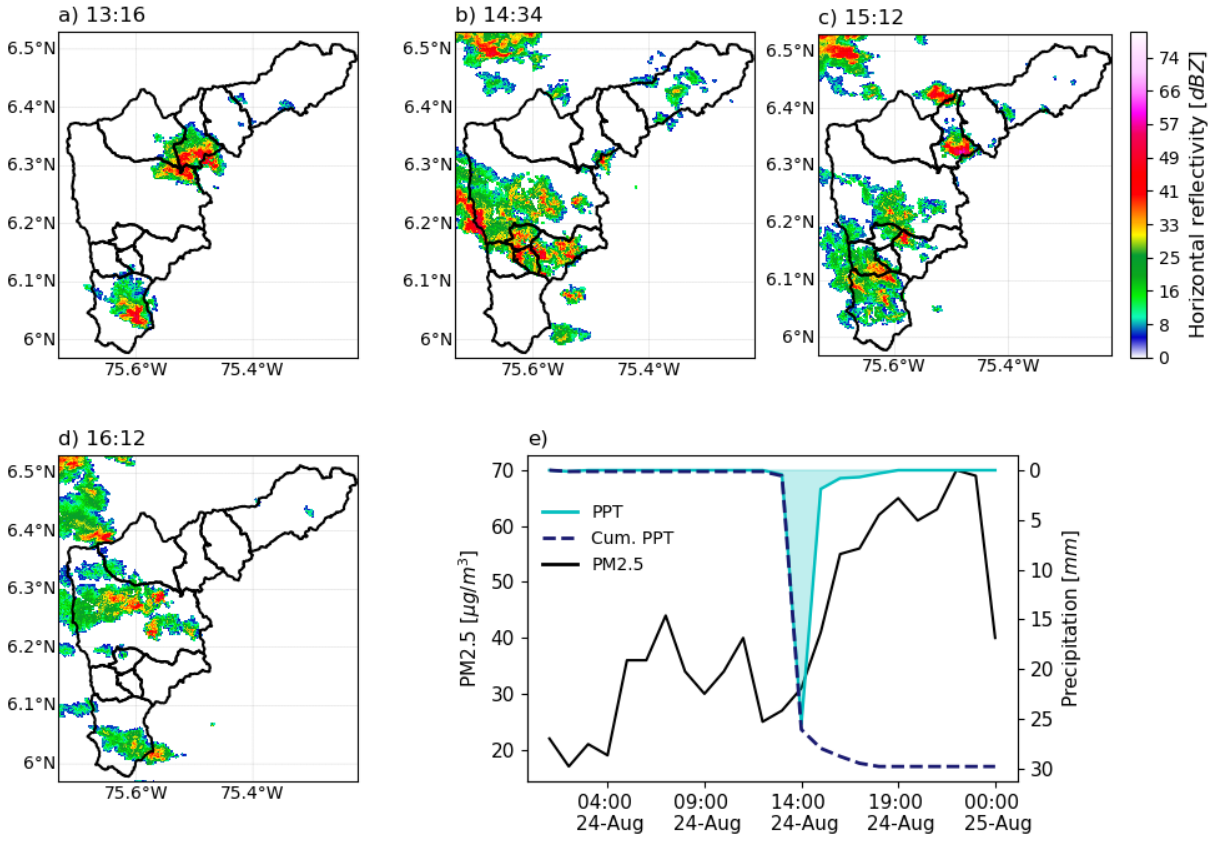

Figura 3-1: a) to d) Radar reflectivity fields as a proxy for the evolution of the precipitation event on August 24, 2016, from 13:00 to 17:30 LT. e) Temporal variability of fine particulate matter (black line), rainfall (blue line), and cumulative rainfall (dashed line).

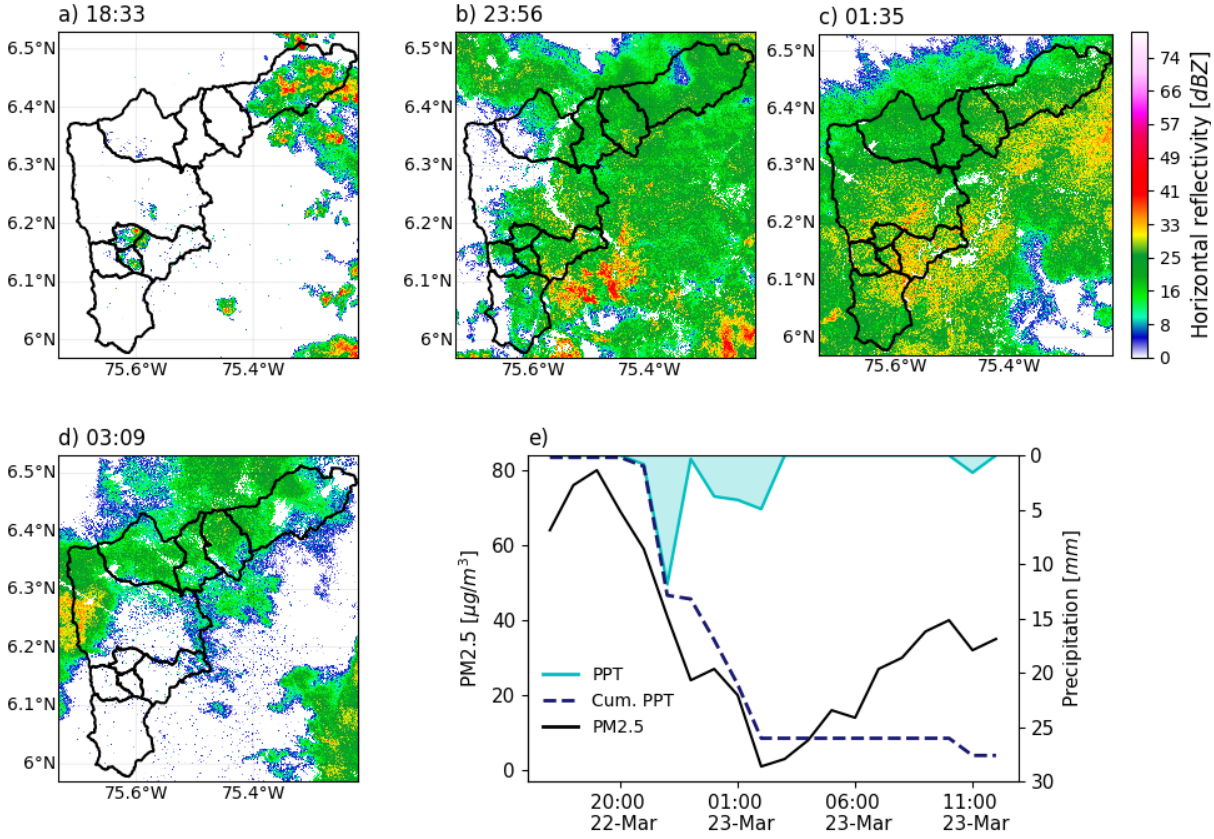

Figura 3-2: Similar as Figure **3-1** for the precipitation event on March 22-23, 2017.

The overall results indicate that the net effect of precipitation during the night is the reduction of particular matter concentration, most likely associated with washout aerosol removal. During the day, between 10:00 and 17:00 LT, the indirect net effect of precipitation is the opposite, leading to an increase in particulate matter concentration. Since the BCS does not depend on whether the precipitation is nocturnal or during the day, other processes must be indirectly offsetting the BCS effect. The comparison between the net rainfall effect in PM2.5 and PM10 hints to a relevant difference regarding particle size. While the overall results for PM2.5 and PM10 are similar, there is an important difference in the 10:00 - 17:00 LT period. During this time, for PM10, the period with positive SOCC index is shorter (10:00 to 15:00 LT) compared to the period for PM2.5 (10:00 to 17:00 LT) and, more importantly, the null

hypothesis cannot be rejected, except at 14:00 and 15:00 LT, and the differences among the PM10 PDFs for wet and dry cases are not significant. This could be related to the aerosol diameter, as the removal efficiency of coarser particles in the 1-10 μm^{-3} range is higher than for finer ones. The previous result is common for all monitoring sites. Figure **3-5**a and b summarize the SOCC index for PM2.5 and PM10, respectively, for all PM monitoring stations in Figure **1-1**, showing a coherent change in SOCC sign during the diurnal cycle associated with net particulate matter removal during the night hours, and net aerosol concentration increase during the day, in wet conditions. Similarly, the precipitation effects on PM10 concentration are weaker, and the null hypothesis cannot be rejected, in the period between midmorning and before the sunset, potentially due to particle size effects.

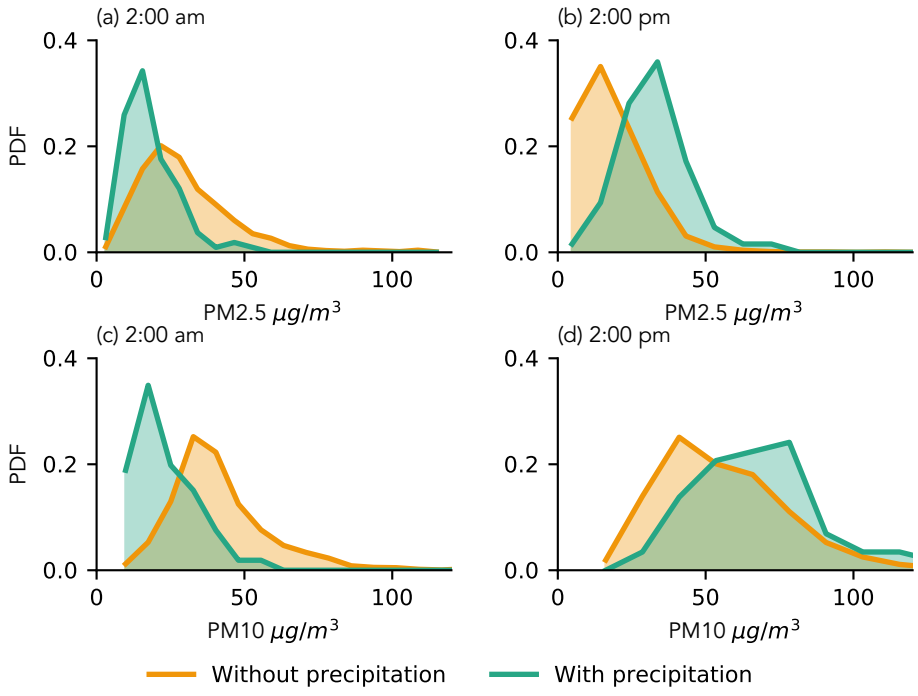

Figura 3-3: PM2.5 concentration PDFs for wet (green line) and dry (orange line) conditions in monitoring station 4 in Figure **1-1** at a) 02:00 LT and b) 14:00 LT. c) and d) Similar to a) and b) for PM10 in monitoring station 5 in Figure **1-1**.

The SOCC index is also used to analyze the effects of cumulative precipitation on aerosol concentration. Figure **3-6** shows, for the 5:00 LT period, at monitoring station 10 (see

Figure **1-1**), the SOCC index for different values of cumulative precipitation. As observed, while the cumulative precipitation increases the value of the SOCC index becomes more negative, i.e. the differences between PDFs for wet and dry conditions are greater, indicating that the net aerosol removal is larger. Thus, as the cumulative precipitation increases, the effects of precipitation are more significant. This is true for both PM2.5 and PM10; however, precipitation removal effects for PM10 are more significant, showing the dependence of wet deposition in aerosol size. The removal efficiency quickly stabilizes as cumulative precipitation reaches 5 mm implying that most aerosol BCS occurs during the first stages of precipitation. Differences between PM10 and PM2.5 washout is explained considering the theory of collision efficiency between particles and rain droplets. According to previous studies, the collection efficiencies is minimum for particles with an aerodynamic diameter roughly between 50 nm and 2 μm [Quérel et al., 2014, Cherrier et al., 2017]; these particles are in the so-called Greenfield Gap [Greenfield, 1957].

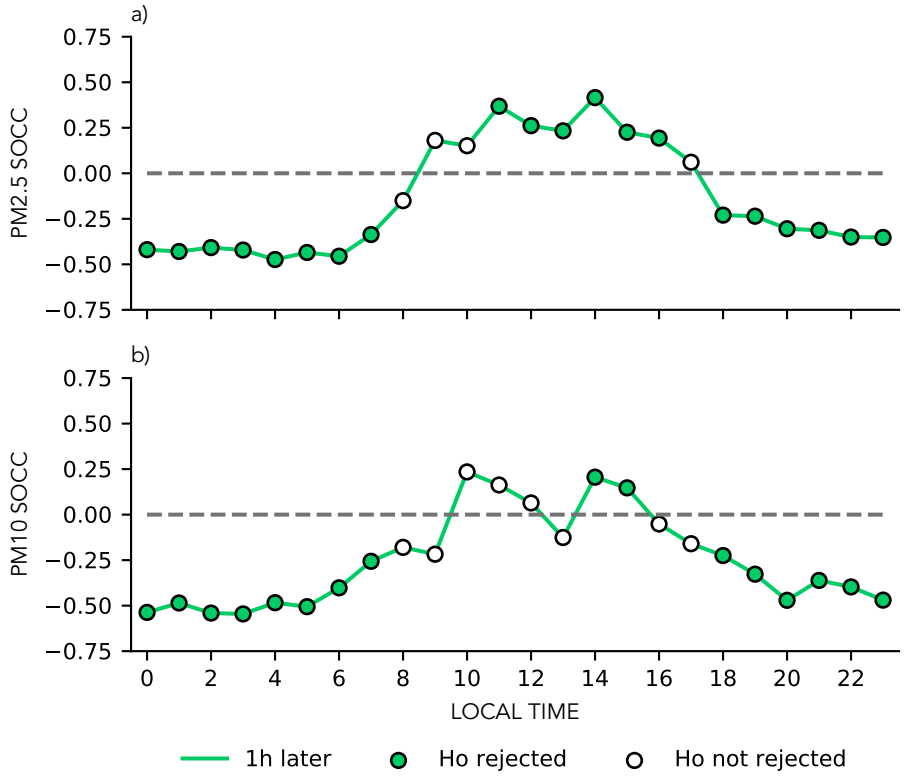

Figura 3-4: Diurnal cycle of the SOCC index for a) PM2.5 in monitoring station 4 and b) PM10 in monitoring station 5. Negative values indicate a net precipitation-induced aerosol removal, and positive ones suggest that precipitation leads to pollution accumulation. Full green circles correspond to cases where the null hypothesis, indicating that the distributions of pollutants for wet and dry conditions are identical, can be rejected using the Wilcoxon-Mann-Whitney test. Conversely, white circles correspond to hours in which the null hypothesis cannot be rejected.

The evidence presented suggests that the role of precipitation in aerosol concentration is strongly dependent on the diurnal cycle of the state of the atmosphere, and in particular, of the atmospheric stability, with positive SOCC index corresponding to times during the day in which the lower troposphere is typically unstable within the valley. Evidence in Figure **3-4** shows that around the transition times between atmospheric stability and instability

(9:00-10:00 am and 5:00-6:00 pm, respectively) the null hypothesis cannot be rejected, indicating that during these periods the differences in aerosol concentration in wet and dry conditions are not statistically significant, and that there is no certainty about the effects of precipitation over aerosol concentrations. Thermodynamic indices are used to evaluate the effect of precipitation event on the lower troposphere stability following the same conditional methodology.

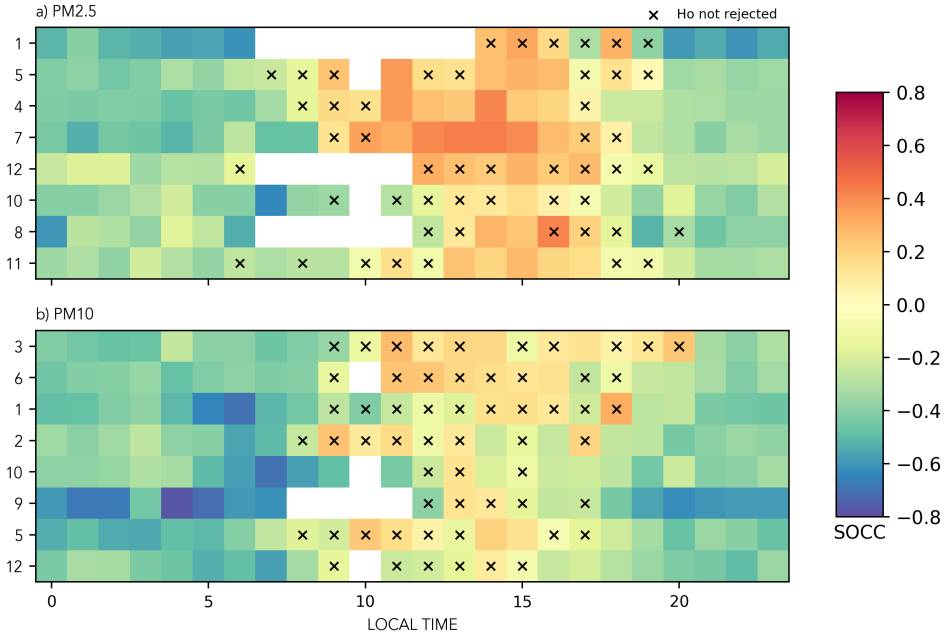

Figura 3-5: Summary of the SOCC index for all a) PM2.5 and b) PM10 stations. White squares correspond to hours of the day where there are no sufficient precipitation cases to estimate statistically significant SOCC index; X marks correspond to cases where null hypothesis, indicating that the distributions of pollutants for wet and dry conditions are identical, cannot be rejected. Numbers in the left correspond to stations in Figure **1-1**.

Figures **3-7** present the PDFs of CINE and LI, for wet and dry conditions, and for 02:00 and 14:00 LT, respectively. It is important to mention that while CINE represents the inhibition of local convection, from bottom-to-top, LI corresponds to a mid-tropospheric index. Figure **3-7**a presents CINE PDFs for 02:00 LT, showing that, at this time, the CINE distribution for wet and dry cases are quite similar. On the contrary, at 14:00 LT (Figure **3-**

7b), results suggest that the CINE PDF for wet conditions is considerably different than for dry conditions, with larger negative values, indicating a lower troposphere stabilization as a result of the precipitation event occurring during unstable conditions. Diurnal precipitation leads to atmospheric stratification, hence decreasing the occurrence of vertical updrafts. The main stabilization mechanism, in a topographically constrained environment, is associated with the formation of a convective cold pool due to evaporatively cooled air transported to the surface through convective downdrafts, modifying the thermodynamic properties and moisture structure in the sub-cloud layer, and generating stable stratification [Simpson, 1969, Charba, 1974, Tompkins, 2001]. Atmospheric stabilization restricts the rise of pollutants from the surface and over the top of the valley (where they can be advected away by the trade winds), leading to pollutant accumulation within the valley, in association with the continued anthropogenic emissions. During the night, and considering that rainfall occurs already in a stratified environment, precipitation does not have a significant effect on atmospheric stability and, in consequence, the CINE PDF does not change between wet and dry cases.

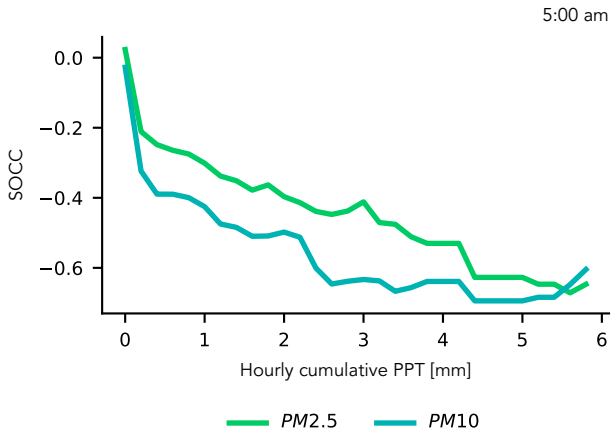

Figura 3-6: SOCC index for different hourly cumulative precipitation at 5:00 LT, for PM2.5 (green line) and PM10 (blue line).

Figure **3-7**c and d show LI distributions for 02:00 and 14:00 LT. Results at both times suggest a slight change towards a more stable atmosphere immediately after the precipitation event. Results differ from the CINE PDFs for 02:00 LT: while CINE PDFs for this period do no evidence any change, LI PDF shows a more stable atmospheric column. The observed

difference is likely to be associated with the nature of both indices: precipitation does appear to influence mid-troposphere stability even if the atmosphere is already stable, most likely associated with the release of latent heat, while it does not seem to affect lower troposphere stability.

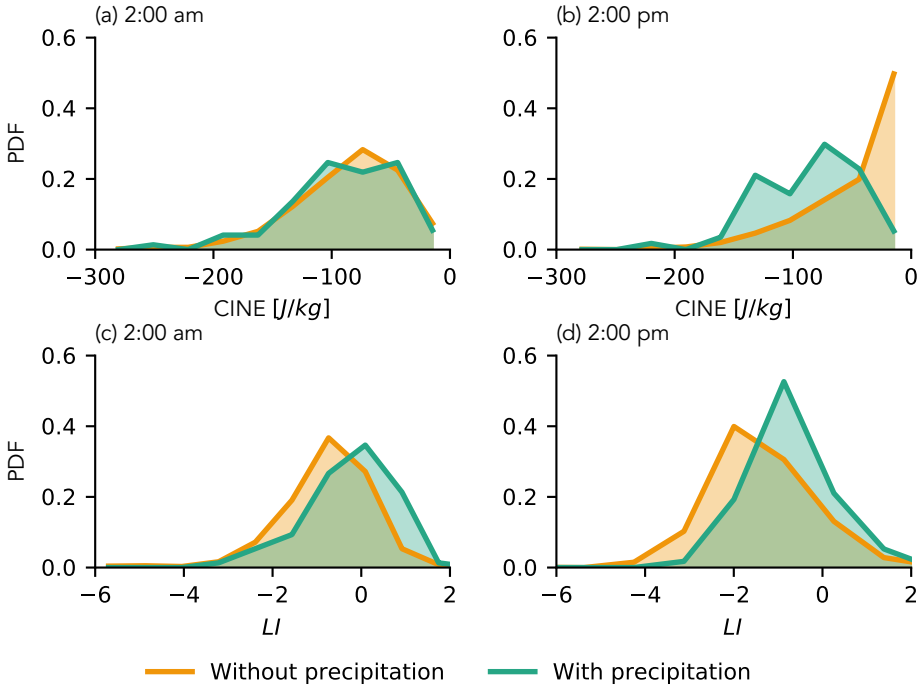

Figura 3-7: CINE PDFs at a) 2:00 LT and b) at 14:00 LT for for wet (green line) and dry (orange line) conditions. c) and d) is the same as a) and b) for LI.

Figure **3-8**a presents an assessment of the role of precipitation intensity in aerosol removal. The figure shows the PDFs of PM2.5, both in wet conditions, for high and low precipitation intensity, using the median intensity as a threshold to separate the full set. The PM2.5 concentration is, in general, lower after low-intensity precipitation events than after high-intensity cases. Before concluding about the higher efficiency of low-intensity events, it is important to consider that, in general, convective systems over the Aburrá Valley occur during the afternoon hours, and are characterized by their high-intensity and short life cycles. Stratiform systems occur mainly during the night hours and are characterized by being of long-lived and their low/medium intensity. Figure **3-8**b presents the distribution

of precipitation intensity for all wet cases, the median precipitation intensity used as a threshold to separate low intensity from high-intensity cases, and the intensity distribution for nighttime and daytime precipitation. The figure shows evidence suggesting a different precipitation intensity distribution depending on the period of the day, also indicating that low PM2.5 concentrations do not depend on the intensity, but, again, on the time of the precipitation. Thus, the apparent role of precipitation intensity is most likely related to the varying net effect of precipitation on aerosol concentration during the course of the day.

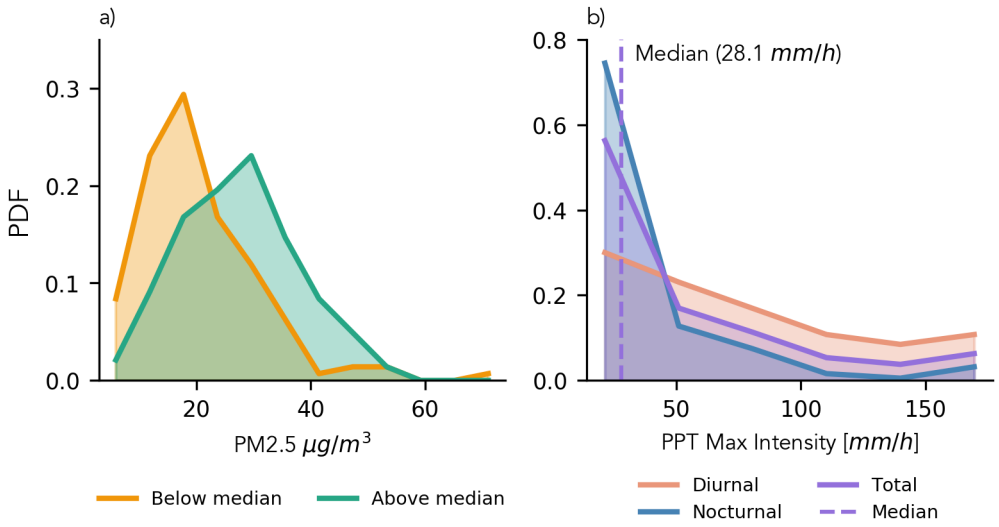

Figura 3-8: a) PDFs of PM2.5 concentration, both in wet conditions, for high (green line) and low (orange line) precipitation intensity. The median intensity is used as a threshold to separate the full set. b) Distribution of precipitation intensity for all wet cases (purple line), median precipitation intensity (vertical line) used as a threshold to separate among low and high-intensity cases, and the intensity distribution for nighttime (blue line) and daytime (coral line) precipitation.

In general, precipitation in the valley presents a very marked diurnal cycle, with two peaks, one of them around 01:00 LT, and the other around 15:00 LT [Poveda et al., 2005], as observed in the continuous black line in Figure **3-9**a. As a result of the divergent effects of nighttime and daytime precipitation on aerosol concentration, the month-to-month variability of the

diurnal cycle of precipitation strongly modulates the air quality, partly determining the likelihood of occurrence of critical air quality episodes. The monthly precipitation over the Aburrá Valley also shows a pronounced annual cycle of precipitation (see Figure **3-9**b), and a bimodal structure as a result of the seasonality of the Intertropical Convergence Zone (ITCZ), with high precipitation during March-April-May (MAM) and September-October-November (SON). In spite of the regularity, the diurnal cycle of precipitation changes considerably from year to year and from month to month. Figure **3-9**a presents the diurnal cycle of precipitation during March, 2016 and 2017, and the historical mean for the month. It is evident that, in addition to the differences in total precipitation, March 2016, was characterized by afternoon convective precipitation, while nighttime precipitation was negligible. Based on the results of the present study, the precipitation diurnal cycle is one of the main factors determining the March 2016, critical air quality episode shown in Figure **3-9**d. The peak in aerosol concentration during the transition season in March 2016, is not observed during October 2016 nor during March 2017, the two following transition seasons. During October 2016, the precipitation diurnal cycle exhibits considerable overnight rainfall (Figure **3-9**c) leading to a net aerosol removal compared to the circumstances during March 2016. Similarly, March 2017 nighttime precipitation was also considerably larger than during March 2016, helping to control, together with the implementation of restrictive emission policies, a sudden increase in aerosol concentrations. These results emphasize the need for a better understanding, and skillful forecasts, of the seasonal and interannual changes in monthly cumulative daytime and nighttime precipitation.

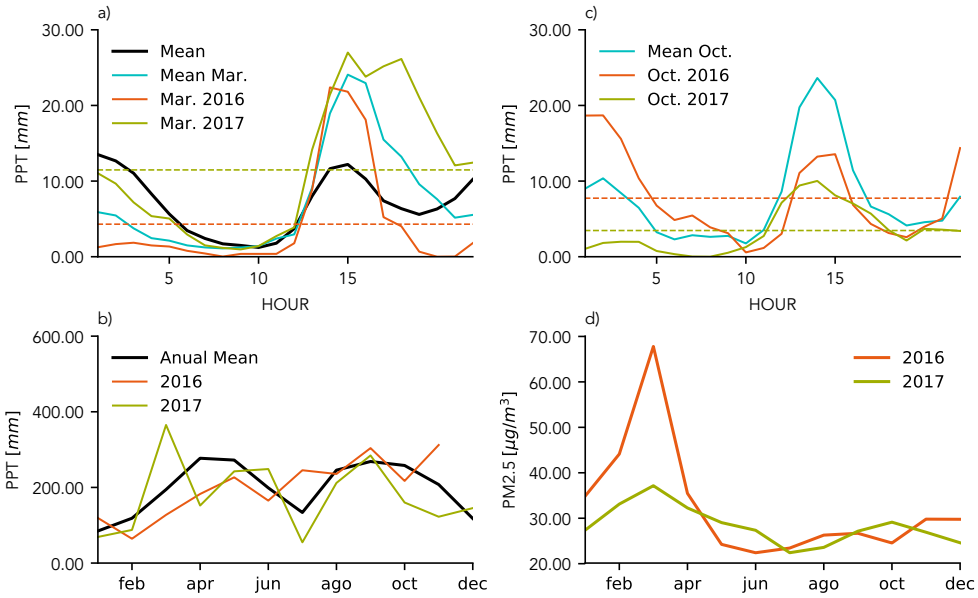

Figura 3-9: Diurnal cycles of precipitation in the Aburrá valley a) for the entire period (black line), the month of March (blue line), March 2016 (orange line), March 2017 (lime line), c) the month of October (blue line), October 2016 (orange line) and October 2017 (lime line). b) Annual cycle of precipitation over the Aburrá Valley (black line), and monthly precipitation during 2016 (orange line) and 2017 (lime line). d) Monthly PM2.5 concentration during 2016 (orange line) and 2017 (lime line).

Precipitation, and the associated atmospheric stabilization, also play an important role in modulating gaseous pollution at certain times of the day. Figures **3-10**a and b present, using data from monitoring station 4 in Figure **1-1**, the NO_2 and Ozone PDFs for wet (blue line) and dry (orange line) conditions at 02:00 and 14:00 LT, respectively. At 02:00 LT, the PDFs for wet and dry conditions are very similar indicating that, in the selected monitoring station, the nighttime rainfall does not have an important effect on the concentration of NO_2 and ozone. In other words, nighttime precipitation does not appear to be an important discriminating factor for NO_2 and ozone concentrations. In the afternoon, at 14:00 LT, however, there is a marked difference between the PDFs of NO_2 and Ozone concentrations in wet and dry conditions. In the case of NO_2, similar to the results for particulate matter with day-

time precipitation, the figure shows a significant increase in NO_2 after precipitation. Both, primary particulate matter and NO_2 are emitted directly from mobile and fixed sources. In the Aburrá Valley, approximately 80% of the direct emissions originate from mobile sources [Universidad Pontificia Bolivariana and Área Metropolitana del Valle de Aburrá, 2017]. As shown before, afternoon rainfall stratifies the lower troposphere, generating the conditions for accumulation of primary pollutants from sustained anthropogenic emissions.

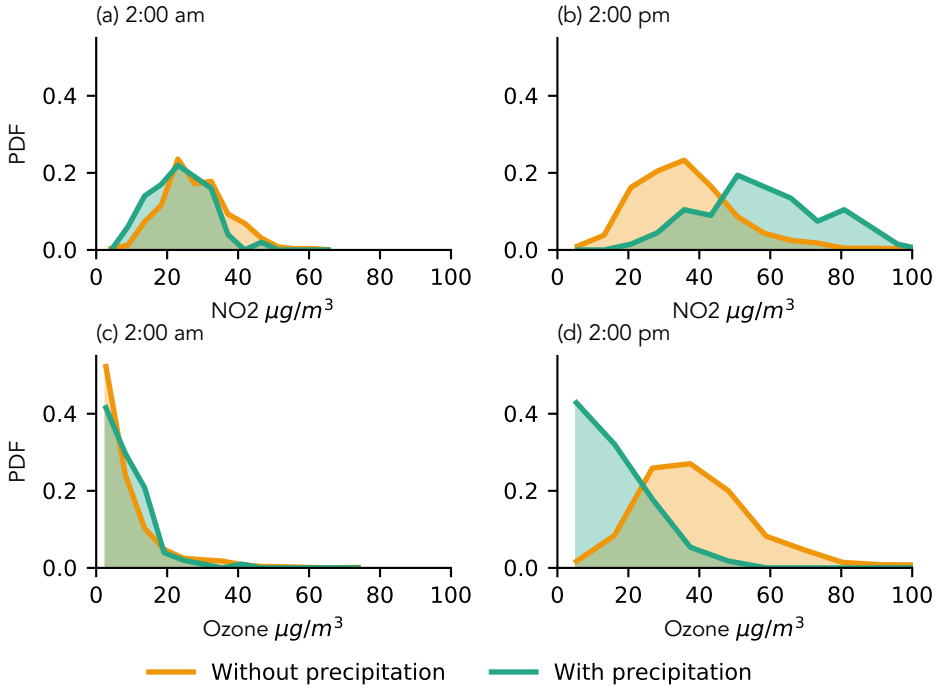

Figura 3-10: Same as Figure **3-3** for NO_2 and Ozone in monitoring station 5.

Other pollutants form in the atmosphere as a result of chemical reactions of precursors in the presence of sunlight and liquid water. Tropospheric ozone, for example, forms when nitrogen oxides, carbon monoxide, and volatile organic compounds, react in the presence of ultraviolet (UV) radiation. Figure **3-10**d presents the PDFs of ozone concentrations for wet and dry conditions; in this case, precipitation leads to low ozone concentrations near the surface as a result of the reduced UV radiation due to the presence of clouds.

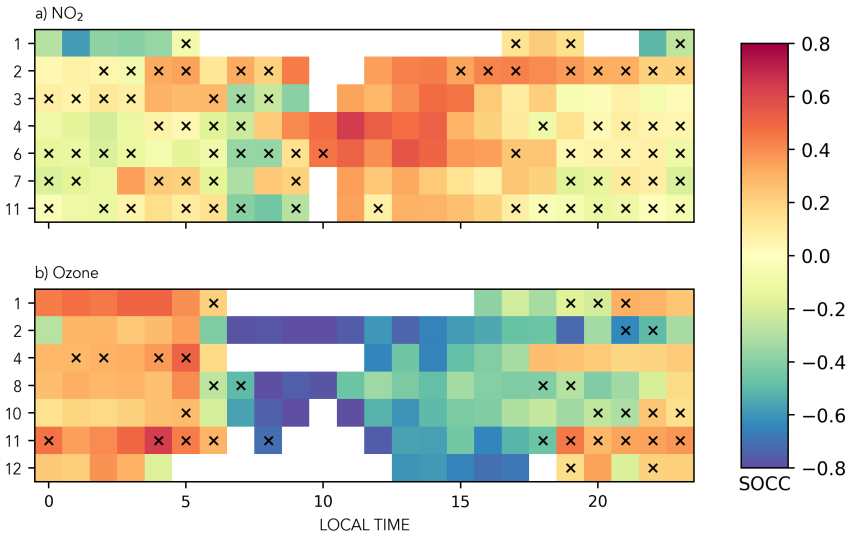

Figura 3-11: Same as Figure **3-5** for NO_2 and Ozone.

The main conclusions regarding the net effects of rainfall on NO_2 and ozone concentration presented for monitoring station 4 in Figure **1-1** are also evident in most monitoring sites. Figure **3-11**a and b summarize the SOCC index for NO_2 and ozone, respectively, for the monitoring stations in Figure **1-1**, also showing a coherent change during the diurnal cycle. In this case, all NO_2 sites show a net accumulation during the daytime after precipitation events, as a result of atmospheric stabilization. During nighttime, the effect is not statistically significant, with no net reduction or accumulation evident in the analysis. On the other hand, all records show evidence of an important ozone formation inhibition during daytime as a result of radiation forcing associated with precipitating clouds. One feature not observed in Figure **3-10**c, and evident in some of the monitoring stations in **3-11**b, is the apparent higher tropospheric ozone concentration after nighttime precipitation relative to during dry conditions. The reason behind the nighttime ozone increments in the valley after precipitation events is not yet clear. The literature suggests different potential mechanisms, among which the most likely is the downward mixing of ozone from the residual layer to the surface, forced by gustiness associated with the formation of a cold pool and frictional vertical mixing caused by droplet fall [Samson, 1978, Klein et al., 2014].

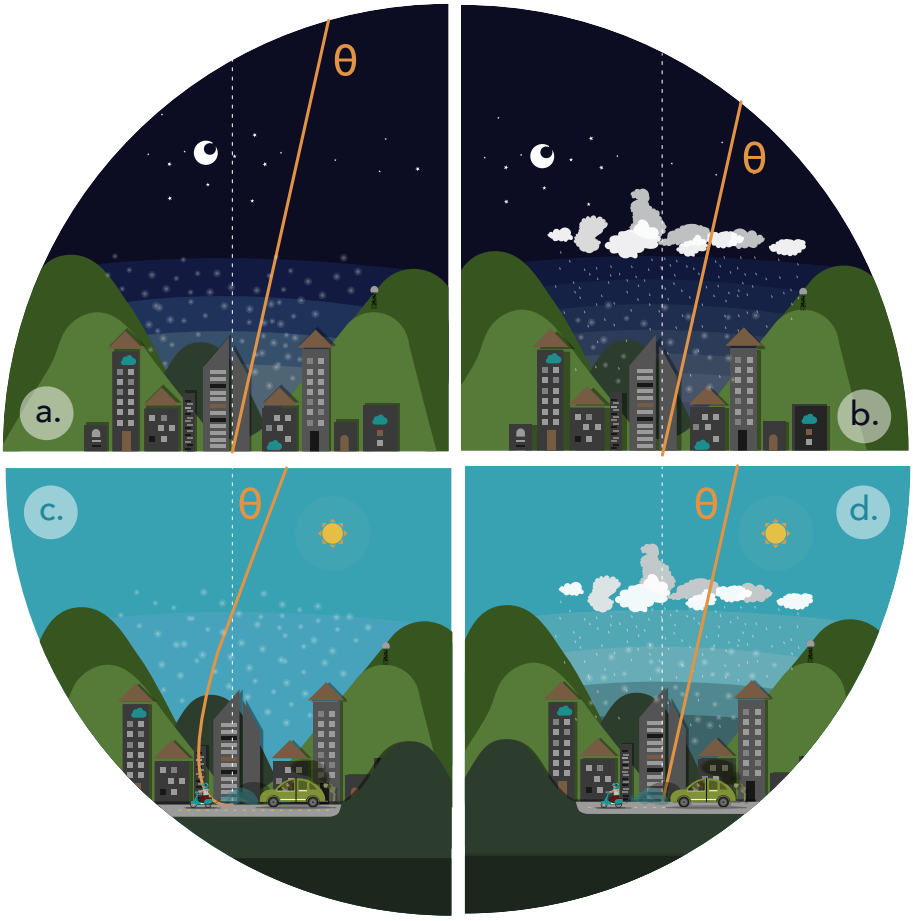

Figura 3-12: Schematic diagram summarizing the net effect of precipitation on pollutant concentration. a) During the nighttime and before midmorning, the potential temperature increases with height indicating the atmosphere is stable; b) a precipitation event during this time generates below cloud scavenging reducing the concentration of particulate matter in the atmosphere. The nighttime precipitation event slightly stabilizes the mid-troposphere, but the near-surface troposphere stability does not change considerably. c) During afternoon hours unstable atmospheric conditions are dominant as represented by the potential temperature profile; convective processes are triggered, and aerosols disperse vertically and away from the valley surface generating a considerable reduction in primary pollutant concentration; however, d) rainfall stabilizes the atmosphere, generating early stratification. Meanwhile, anthropogenic emis-

4 Conclusions

The present work introduces an alternative observational methodology to study the processes associated with wet deposition, and more generally, with the net effect of precipitation in pollution concentration near the surface, adding to the important microphysical approach that has been key in the fields of air-quality and cloud formation. The methodology, a non-parametric conditional analysis using a signed overlapping coefficient complement (SOCC), allows assessing the net effect of precipitation on pollutant concentration considering not only the direct near-surface aerosol removal effect associated with below-cloud scavenging but also the indirect effect associated with the induced changes in the lower troposphere leading to pollutant concentration. In particular, daytime precipitation alters the lower troposphere inducing near-surface stability, which in turns affect the dispersion or pollutants.

Net effects of precipitation on pollutant concentrations were studied using the monitoring stations located in the Aburrá Valley metropolitan area, considering different times during the day. Results of the study suggest that the effects of precipitation on PM2.5, PM10 are NO_2 are strongly dependent on the atmospheric stability. Figure **3-12** presents a schematic diagram summarizing the main results. During the nighttime (see Figure **3-12**a) and before midmorning, the potential temperature increases with height indicating the atmosphere is stable; a precipitation event during this time generates below cloud scavenging reducing the concentration of particulate matter in the atmosphere (see Figure **3-12**b); NO_2 concentration remains unchanged, and in some cases ozone increases after the event. The nighttime precipitation event slightly stabilizes the mid-troposphere, but the near-surface troposphere stability does not change considerably (Figure **3-12**b). The mid-tropospheric stabilization is

probably associated with warming as a result of latent heating. Nevertheless, the atmosphere was already stable and the differences are not significant.

During afternoon hours unstable atmospheric conditions are dominant as represented by the potential temperature profile in Figure **3-12**c; convective processes are triggered, and aerosols disperse vertically and away from the valley surface generating a considerable reduction in primary pollutant concentration; however, rainfall stabilizes the atmosphere, generating early stratification as shown in Figure **3-12**d. The stabilizing effect of rainfall was confirmed based on thermodynamic indices such as CINE and LI. Meanwhile, anthropogenic emissions continue as represented by the vehicles in Figures **3-12**c and d. On a dry day, due to the efficient expansion of the convective boundary layer, pollutant emissions escape the valley. On the contrary, on rainy days the early stratification leads to near-surface pollutant accumulation offsetting the washout effect (Figure **3-12**d); in this case, the net effect of precipitation is to increase primary pollutant concentration (particulate matter and NO_2). The case of ozone is different; reduced radiation associated with clouds inhibits the formation of ozone.

The methodology using the signed overlapping coefficient complement allowed us to detect the contrasting effect of precipitation at different hours of the day as a result of the competing effects of below-cloud scavenging and atmospheric stability. Additionally, it was possible to see that as hourly cumulative precipitation increases, the effects of precipitation are more significant. On the other hand, results indicate that PM10 was more efficiently removed compared to PM2.5, showing the important influence on particulate matter size for the scavenging process. The results also suggest that the year-to-year and month-to-month varying precipitation diurnal cycle modulates the annual cycle of particulate matter concentration, in particular, PM2.5. This finding underlines the need to study in detail the interannual and long-term variability of the precipitation diurnal cycle; while there is significant research on the interannual precipitation variability in a monthly timescale, not enough research has focused on the longterm variability of the sub-daily structure of rainfall, including the frequency of convective vs. stratiform precipitation locally.

The results of this work are useful not only for a better understanding of the general mechanisms controlling pollutant accumulation near the surface but also as a tool for policy-makers regarding decisions related to air quality control via emission restrictions to avoid sudden critical air quality episodes in the midst of environments characterized by prevalent atmospheric stability and scarce nighttime rainfall, allowing the development of better environmental policies for management, prevention and mitigation of air pollution around cities.

Bibliography

Paula A. Agudelo, Carlos D. Hoyos, Judith A. Curry, and Peter J. Webster. Probabilistic discrimination between large-scale environments of intensifying and decaying african easterly waves. *Climate Dynamics*, 36(7):1379–1401, Apr 2011. ISSN 1432-0894. doi: 10.1007/s00382-010-0851-x. URL https://doi.org/10.1007/s00382-010-0851-x.

Jonathan O. Anderson, Josef G. Thundiyil, and Andrew Stolbach. Clearing the Air: A Review of the Effects of Particulate Matter Air Pollution on Human Health. *Journal of Medical Toxicology*, 8(2):166–175, 2012. ISSN 15569039. doi: 10.1007/s13181-011-0203-1.

C Andronache and Chestnut Hill. Estimated variability of below-cloud aerosol removal by rainfall for observed aerosol size distributions. *Atmospheric Chemistry and Physics*, 3: 131–143, 2003.

Soo Ya Bae, Rokjin J. Park, Yong Pyo Kim, and Jung Hun Woo. Effects of below-cloud scavenging on the regional aerosol budget in East Asia. *Atmospheric Environment*, 58:14–22, 2012. ISSN 13522310. doi: 10.1016/j.atmosenv.2011.08.065. URL http://dx.doi.org/10.1016/j.atmosenv.2011.08.065.

Carlos Blanco-Alegre, Amaya Castro, Ana I. Calvo, Fernanda Oduber, Elisabeth Alonso-Blanco, Delia Fernández-González, Rosa M. Valencia-Barrera, Ana M. Vega-Maray, and Roberto Fraile. Below-cloud scavenging of fine and coarse aerosol particles by rain: The role of raindrop size. *Quarterly Journal of the Royal Meteorological Society*, 0(0). doi: 10.1002/qj.3399. URL https://rmets.onlinelibrary.wiley.com/doi/abs/10.1002/qj.3399.

Bert Brunekreef and Stephen T. Holgate. Air pollution and health. *Lancet*, 360(9341): 1233–1242, 2002. ISSN 01406736. doi: 10.1016/S0140-6736(02)11274-8.

Jess Charba. Application of gravity current model to analysis of squall-line gust front. *Monthly Weather Review*, 102(2):140–156, 1974. doi: 10.1175/1520-0493(1974)102¡0140:AOGCMT¿2.0.CO;2. URL `https://doi.org/10.1175/1520-0493(1974)102<0140:AOGCMT>2.0.CO;2`.

D. M. Chate and T. S. Pranesha. Field studies of scavenging of aerosols by rain events. *Journal of Aerosol Science*, 35(6):695–706, 2004. ISSN 00218502. doi: 10.1016/j.jaerosci.2003.09.007.

D. M. Chate, P. Murugavel, K. Ali, S. Tiwari, and G. Beig. Below-cloud rain scavenging of atmospheric aerosols for aerosol deposition models. *Atmospheric Research*, 99(3-4):528–536, 2011. ISSN 01698095. doi: 10.1016/j.atmosres.2010.12.010. URL `http://dx.doi.org/10.1016/j.atmosres.2010.12.010`.

Abhijit Chatterjee, Achutan Jayaraman, T. Narayana Rao, and Sibaji Raha. In-cloud and below-cloud scavenging of aerosol ionic species over a tropical rural atmosphere in India. *Journal of Atmospheric Chemistry*, 66(1-2):27–40, 2010. ISSN 01677764. doi: 10.1007/s10874-011-9190-5.

Zhen Cheng, Lina Luo, Shuxiao Wang, Yungang Wang, Sumit Sharma, Hikari Shimadera, Xiaoliang Wang, Michael Bressi, Regina Maura de Miranda, Jingkun Jiang, Wei Zhou, Oscar Fajardo, Naiqiang Yan, and Jiming Hao. Status and characteristics of ambient PM2.5pollution in global megacities. *Environment International*, 89-90:212–221, 2016. ISSN 18736750. doi: 10.1016/j.envint.2016.02.003. URL `http://dx.doi.org/10.1016/j.envint.2016.02.003`.

Gaël Cherrier, Emmanuel Belut, Fabien Gerardin, Anne Tanière, and Nicolas Rimbert. Aerosol particles scavenging by a droplet: Microphysical modeling in the Greenfield gap. *Atmospheric Environment*, 166:519–

530, 2017. ISSN 18732844. doi: 10.1016/j.atmosenv.2017.07.052. URL http://dx.doi.org/10.1016/j.atmosenv.2017.07.052.

J.A. Curry and P.J. Webster. *Thermodynamics of Atmospheres and Oceans*. International Geophysics. Elsevier Science, 1999. ISBN 9780121995706. URL https://books.google.com.co/books?id=mdFzlFfWbiYC.

By Venita Depuy, Vance W Berger, and Yanyan Zhou. Wilcoxon-Mann-Whitney Test: Overview. *Wiley StatsRef: Statistics Reference Online*, pages 1–5, 2014. doi: 10.1002/9781118445112.stat06547.

Nora Duhanyan and Yelva Roustan. Below-cloud scavenging by rain of atmospheric gases and particulates. *Atmospheric Environment*, 45(39):7201–7217, 2011. ISSN 13522310. doi: 10.1016/j.atmosenv.2011.09.002. URL http://dx.doi.org/10.1016/j.atmosenv.2011.09.002.

Hamdy K. Elminir. Dependence of urban air pollutants on meteorology. *Science of the Total Environment*, 350(1-3):225–237, 2005. ISSN 00489697. doi: 10.1016/j.scitotenv.2005.01.043.

Jian Feng. A 3-mode parameterization of below-cloud scavenging of aerosols for use in atmospheric dispersion models. *Atmospheric Environment*, 41:6808–6822, 2007. doi: 10.1016/j.atmosenv.2007.04.046.

Xinyuan Feng and Shigong Wang. Influence of different weather events on concentrations of particulate matter with different sizes in Lanzhou, China. *Journal of Environmental Sciences*, 24(4):665–674, 2012. ISSN 1001-0742. doi: 10.1016/S1001-0742(11)60807-3. URL http://dx.doi.org/10.1016/S1001-0742(11)60807-3.

Stanley Marshall Greenfield. Rain scavenging of radioactive particulate matter from the atmosphere. *Journal of Meteorology*, 14(2):115–125, 1957.

Nancy B. Grimm, Stanley H. Faeth, Nancy E. Golubiewski, Charles L. Redman, Jianguo Wu, Xuemei Bai, and John M. Briggs. Global change and the ecology of cities. *Sci-*

ence, 319(5864):756–760, 2008. ISSN 0036-8075. doi: 10.1126/science.1150195. URL http://science.sciencemag.org/content/319/5864/756.

Ling Chuan Guo, Lian Jun Bao, Jian Wen She, and Eddy Y. Zeng. Significance of wet deposition to removal of atmospheric particulate matter and polycyclic aromatic hydrocarbons: A case study in Guangzhou, China. *Atmospheric Environment*, 83:136–144, 2014. ISSN 18732844. doi: 10.1016/j.atmosenv.2013.11.012. URL http://dx.doi.org/10.1016/j.atmosenv.2013.11.012.

Ling-chuan Guo, Yonghui Zhang, Hualiang Lin, Weilin Zeng, Tao Liu, Jianpeng Xiao, Shannon Rutherford, Jing You, and Wenjun Ma. The washout effects of rainfall on atmospheric particulate pollution in two Chinese cities. *Environmental Pollution*, 215:195–202, 2016. ISSN 0269-7491. doi: 10.1016/j.envpol.2016.05.003. URL http://dx.doi.org/10.1016/j.envpol.2016.05.003.

Henry F. Inman and Edwin L. Bradley. The Overlapping Coefficient as a Measure of Agreement Between Probability Distributions and Point Estimation of the Overlap of two Normal Densities. *Communications in Statistics - Theory and Methods*, 18(10):3851–3874, 1989. ISSN 1532415X. doi: 10.1080/03610928908830127.

Petra M. Klein, Xiao-Ming Hu, and Ming Xue. Impacts of mixing processes in nocturnal atmospheric boundary layer on urban ozone concentrations. *Boundary-Layer Meteorology*, 150(1):107–130, Jan 2014. ISSN 1573-1472. doi: 10.1007/s10546-013-9864-4. URL https://doi.org/10.1007/s10546-013-9864-4.

Ella Maria Kyrö, Tiia Grönholm, Henri Vuollekoski, Aki Virkkula, Markku Kulmala, and Lauri Laakso. Snow scavenging of ultrafine particles: Field measurements and parameterization. *Boreal Environment Research*, 14(4):527–538, 2009. ISSN 12396095.

Philip J. Landrigan, Richard Fuller, Nereus J.R. Acosta, Olusoji Adeyi, Robert Arnold, Niladri Basu, Abdoulaye Bibi Baldé, Roberto Bertollini, Stephan Bose-O'Reilly, Jo Ivey Boufford, Patrick N. Breysse, Thomas Chiles, Chulabhorn Mahidol, Awa M. Coll-Seck, Maureen L. Cropper, Julius Fobil, Valentin Fuster, Michael Greenstone, Andy Haines,

David Hanrahan, David Hunter, Mukesh Khare, Alan Krupnick, Bruce Lanphear, Bindu Lohani, Keith Martin, Karen V. Mathiasen, Maureen A. McTeer, Christopher J.L. Murray, Johanita D. Ndahimananjara, Frederica Perera, Janez Potočnik, Alexander S. Preker, Jairam Ramesh, Johan Rockström, Carlos Salinas, Leona D. Samson, Karti Sandilya, Peter D. Sly, Kirk R. Smith, Achim Steiner, Richard B. Stewart, William A. Suk, Onno C.P. van Schayck, Gautam N. Yadama, Kandeh Yumkella, and Ma Zhong. The Lancet Commission on pollution and health. *The Lancet*, 6736(17), 2017. ISSN 1474547X. doi: 10.1016/S0140-6736(17)32345-0.

Mihalis Lazaridis. First principles of meteorology. In *First Principles of Meteorology and Air Pollution*, pages 67–118. Springer, 2011.

J. Lelieveld, J. S. Evans, M. Fnais, D. Giannadaki, and A. Pozzer. The contribution of outdoor air pollution sources to premature mortality on a global scale. *Nature*, 525(7569): 367–371, 2015. ISSN 14764687. doi: 10.1038/nature15371.

Han Li, Bin Guo, Mengfei Han, Miao Tian, and Jin Zhang. Particulate matters pollution characteristic and the correlation between pm (pm2. 5, pm10) and meteorological factors during the summer in shijiazhuang. *Journal of Environmental Protection*, 6(05):457, 2015.

Mann-Whitney. On a Test of Whether one of Two Random Variables is Stochastically Larger than the Other Author (s): H . B . Mann and D . R . Whitney Source. *The Annals of Mathematical Statistics*, 18(1):50–60, 1947. doi: 10.2307/2236101.

Miriam E. Marlier, Amir S. Jina, Patrick L. Kinney, and Ruth S. DeFries. Extreme Air Pollution in Global Megacities. *Current Climate Change Reports*, 2(1):15–27, 2016. ISSN 21986061. doi: 10.1007/s40641-016-0032-z.

Helmut Mayer. Air pollution in cities. *Atmospheric environment*, 33(24-25):4029–4037, 1999.

Thomas Münzel, Mette Sørensen, Tommaso Gori, Frank P. Schmidt, Xiaoquan Rao, Jeffrey Brook, Lung Chi Chen, Robert D. Brook, and Sanjay Rajagopalan. Environmental stressors and cardio-metabolic disease: Part I-epidemiologic evidence supporting a role for

noise and air pollution and effects of mitigation strategies. *European Heart Journal*, 38 (8):550–556, 2017. ISSN 15229645. doi: 10.1093/eurheartj/ehw269.

David E. Newby, Pier M. Mannucci, Grethe S. Tell, Andrea A. Baccarelli, Robert D. Brook, Ken Donaldson, Francesco Forastiere, Massimo Franchini, Oscar H. Franco, Ian Graham, Gerard Hoek, Barbara Hoffmann, Marc F. Hoylaerts, Nino Künzli, Nicholas Mills, Juha Pekkanen, Annette Peters, Massimo F. Piepoli, Sanjay Rajagopalan, and Robert F. Storey. Expert position paper on air pollution and cardiovascular disease. *European Heart Journal*, 36(2):83–93, 2015. ISSN 15229645. doi: 10.1093/eurheartj/ehu458.

Tomasz Olszowski. Changes in PM10 concentration due to large-scale rainfall. *Arabian Journal of Geosciences*, 9(2):1–11, 2016. ISSN 18667538. doi: 10.1007/s12517-015-2163-2.

Randy A Peppler. A review of static stability indices and related thermodynamic parameters. Technical report, Illinois State Water Survey, 1988.

Germán Poveda, Oscar J. Mesa, Luis F. Salazar, Paola a. Arias, Hernán a. Moreno, Sara C. Vieira, Paula a. Agudelo, Vladimir G. Toro, and J. Felipe Alvarez. The Diurnal Cycle of Precipitation in the Tropical Andes of Colombia. *Monthly Weather Review*, 133(1): 228–240, 2005. ISSN 0027-0644. doi: 10.1175/MWR-2853.1.

Hans R Pruppacher and James D Klett. *Microphysics of Clouds and Precipitation: Reprinted 1980*. Springer Science & Business Media, 2012.

A. Quérel, P. Lemaitre, M. Monier, E. Porcheron, A. I. Flossmann, and M. Hervo. An experiment to measure raindrop collection efficiencies: Influence of rear capture. *Atmospheric Measurement Techniques*, 7(5):1321–1330, 2014. ISSN 18678548. doi: 10.5194/amt-7-1321-2014.

Perry J. Samson. Nocturnal ozone maxima. *Atmospheric Environment (1967)*, 12(4):951 – 955, 1978. ISSN 0004-6981. doi: https://doi.org/10.1016/0004-6981(78)90035-5. URL `http://www.sciencedirect.com/science/article/pii/0004698178900355`.

John H Seinfeld and Spyros N Pandis. *Atmospheric chemistry and physics: from air pollution to climate change*. John Wiley & Sons, 2012.

J. E. Simpson. A comparison between laboratory and atmospheric density currents. *Quarterly Journal of the Royal Meteorological Society*, 95(406):758–765, 1969. doi: 10.1002/qj.49709540609. URL https://rmets.onlinelibrary.wiley.com/doi/abs/10.1002/qj.49709540609.

Adrian M. Tompkins. Organization of tropical convection in low vertical wind shears: The role of cold pools. *Journal of the Atmospheric Sciences*, 58(13): 1650–1672, 2001. doi: 10.1175/1520-0469(2001)058¡1650:OOTCIL¿2.0.CO;2. URL https://doi.org/10.1175/1520-0469(2001)058<1650:OOTCIL>2.0.CO;2.

Universidad Pontificia Bolivariana and Área Metropolitana del Valle de Aburrá. Inventario de emisiones atmosféricas del Valle de Aburrá, actualización 2015. Technical report, Medellín, 2017. URL https://www.epm.com.co/site/Portals/2/ESTUDIOS GNV/Informe_Inventario_emisiones_2015.pdf?ver=2018-05-08-161950-497.

X Wang, L Zhang, and MD Moran. Uncertainty assessment of current size-resolved parameterizations for below-cloud particle scavenging by rain. *Atmospheric Chemistry and Physics*, 10(12):5685–5705, 2010.

C David Whiteman. *Mountain meteorology: fundamentals and applications*. Oxford University Press, 2000.

Yiru Yang, Xingang Liu, Yu Qu, Jingli Wang, Junling An, Yuanhangi Zhang, and Fang Zhang. Formation mechanism of continuous extreme haze episodes in the megacity Beijing, China, in January 2013. *Atmospheric Research*, 155:192–203, 2015. ISSN 01698095. doi: 10.1016/j.atmosres.2014.11.023.

Xin Zhang, Xi Chen, and Xiaobo Zhang. The impact of exposure to air pollution on cognitive performance. *Proceedings of the National Academy of Sciences*, 115(37):9193–9197, 2018.

Nadezda Zikova and Vladimir Zdimal. Precipitation scavenging of aerosol particles at a rural site in the czech republic. *Tellus B: Chemical and Physical Meteorology*, 68(1):27343, 2016.